Journal of Medicinal Chemistry

BRIEF ARTICLE

pubs.acs.org/jmc

Synthesis and Evaluation of Diarylthiazole Derivatives That Inhibit Activation of Sterol Regulatory Element-Binding Proteins

Shinji Kamisuki,[†] Takashi Shirakawa,[†] Akira Kugimiya,[†] Lutfi Abu-Elheiga,[‡] Hea-Young Park Choo,[†,§] Kohei Yamada,[†] Hiroki Shimogawa,[†] Salih J. Wakil,[*,‡] and Motonari Uesugi[*,†,‡]

[†]Institute for Chemical Research and Institute for Integrated Cell-Material Sciences, Kyoto University, Uji, Kyoto 611-0011, Japan

[‡]The Verna and Marrs McLean Department of Biochemistry and Molecular Biology, Baylor College of Medicine, Houston, Texas 77030, United States

Supporting Information

ABSTRACT: Fatostatin, a recently discovered small molecule that inhibits activation of sterol regulatory element-binding protein (SREBP), blocks biosynthesis and accumulation of fat in obese mice. We synthesized and evaluated a series of fatostatin derivatives. Our structure−activity relationships led to the identification of *N*-(4-(2-(2-propylpyridin-4-yl)thiazol-4-yl)phenyl)methanesulfonamide (**24**, FGH10019) as the most potent druglike molecule among the analogues tested. Compound **24** has high aqueous solubility and membrane permeability and may serve as a seed molecule for further development.

INTRODUCTION

Long-chain fatty acids are major sources of energy and important components of the lipids that compose cellular membranes. De novo lipid synthesis is activated in some types of cancers, and synthesized lipids are accumulated in the body in metabolic syndrome. Therefore, pharmacological intervention for de novo lipid synthesis may prove to be effective against a number of human diseases. The conversion of carbohydrates into lipids through de novo fatty acid involves at least 12 enzymatic reactions, and conversion through cholesterol synthesis involves at least 23. Expression levels of the genes encoding these enzymes are controlled by transcription factors, which are designated sterol regulatory element-binding proteins (SREBPs).[1,2] SREBPs are synthesized as ER membrane-bound precursors and must be proteolytically released by two proteases bound to the Golgi membrane (site-1 (S1P) and site-2 (S2P) proteases) to generate forms that activate transcription of target genes in the nucleus.[1,3] Activation of SREBPs is tightly regulated by negative feedback: sterols interact with SREBP cleavage-activating protein (SCAP), an ER membrane-bound escort protein of SREBPs, thereby retaining the SCAP/SREBP complex in the ER.[4,5] Binding of the sterol to SCAP promotes the interaction of SCAP with INSIG, a retention protein in the ER.[6,7] Thus, SREBPs are key lipogenic transcription factors that govern the homeostasis of fat metabolism, and SCAP plays a pivotal role in the regulation of SREBPs.

We previously described a synthetic diarylthiazole molecule fatostatin (**1**, Figure 1) and identified its target. Fatostatin (125B11) was originally discovered from a chemical library as a synthetic small molecule that inhibited insulin-induced adipogenesis and serum-independent growth of cancer cells in cell culture.[8] The molecule was later shown to selectively reduce the expression of SREBP target genes by blocking the activation of SREBP transcription factors.[9] The direct target of fatostatin appears to be SCAP; however, fatostatin does not affect the interaction of SCAP with SREBP-2 or insulin-induced gene (INSIG) and binds to SCAP at a site distinct from that of sterols.[9] Thus, fatostatin is a unique small molecule that blocks the activation of SREBPs independently of INSIG and sterols. Fatostatin or its analogues may serve as research tools for investigating the SREBP/SCAP pathway.

The structure of fatostatin also provides a model that may help direct the design of molecules for pharmacological intervention against cancer progression and metabolic diseases, including fatty liver disease. In fact, fatostatin down-regulated the expression of lipogenic enzymes and blocked increases in body weight, blood glucose, and hepatic fat accumulation in obese ob/ob mice, even under uncontrolled food intake.[9] However, fatostatin showed only moderate potency in mice, and its utility was limited by low aqueous solubility. In this study, we synthesized a number of fatostatin derivatives and compared their potency and physicochemical properties to identify an analogue with improved characteristics for use in further in vivo evaluation in a variety of disease models.

CHEMISTRY

Fatostatin is composed of three aromatic rings: pyridine, thiazole, and toluene. Four routes were used to synthesize fatostatin derivatives (Schemes 1, S1−3 in Supporting Information). In the first route, a central thiazole ring was constructed by reacting various thioamide derivatives with α-bromoketone derivatives (Scheme 1). Thioamide **2** or **3** was coupled with an α-bromoketone precursor in warm ethanol to yield 4-phenyl-2-(pyridin-4-yl)thiazole derivatives (**4**−**9**). The products crystallized directly from the mixtures were filtered to provide high yields of pure thiazoles. Analogue **10** was synthesized by the reaction of **3** with 2-bromo-1-(thiophen-2-yl)ethanone. Diphenylthiazole **12** was

Received: March 17, 2011
Published: May 11, 2011

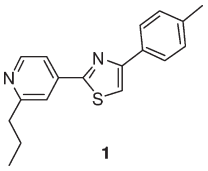

Figure 1. Structure of fatostatin (**1**).

Scheme 1. Synthesis of Analogues 4−10, 12

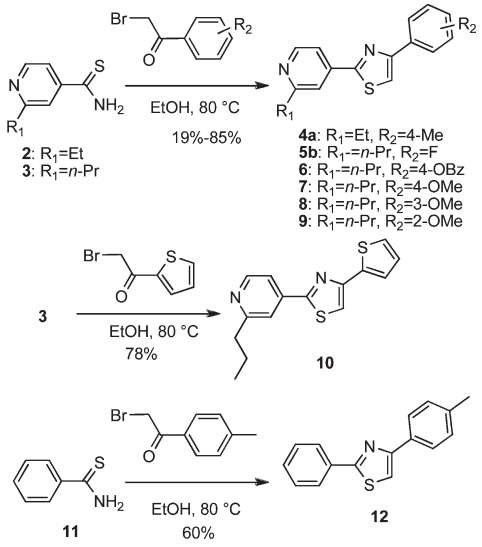

similarly synthesized from benzothioamide (**11**) and 2-bromo-1-*p*-tolylethanone.

To prepare analogue **15**, 4-bromo-2-propylpyridine (**14**) was first synthesized from 4-bromopyridine (**13**), as previously described.[10] Suzuki coupling of bromide **14** with 4′-methyl-4-biphenylboronic acid produced analogue **15** (Scheme S1).

Phenol derivatives (Scheme S2) were prepared by alkaline hydrolysis of analogue **6**, producing the *p*-phenol derivative **16**, or demethylation of methyl ether **8** and **9** by BBr_3, producing the *m*-phenol derivative **17** and *o*-phenol derivative **18**.

Amine, amide, and sulfonamide derivatives were also synthesized (Scheme S3). Isopropylamine **20**, benzylamine **21**, and cyclopropylmethylamine **22** were prepared in high yields by a direct reductive amination reaction of acetone, benzaldehyde, or cyclopropanecarboxaldehyde with a previously prepared primary amine **19**.[11] Amine **19** was also reacted with acetyl chloride, methanesulfonyl chloride, thiophenesulfonyl chloride, or tosyl chloride in the presence of pyridine to yield acetoamide **23**, methanesulfoneamide **24**, thiophenesulfoneamide **25**, or toluenesulfoneamide **26**, respectively.

RESULTS AND DISCUSSION

All of the synthesized fatostatin derivatives were assayed for their ability to inhibit the expression of a luciferase reporter gene, in which expression of luciferase was controlled by three repeats of sterol regulatory elements (SREs). This SREBP-responsive reporter construct was co-transfected into Chinese hamster ovary K1 (CHO-K1) cells with a control β-gal reporter gene in which the expression of β-gal was driven by a constitutively active actin promoter. Luciferase expression from the SREBP-responsive reporter gene, normalized to β-gal expression, was activated upon lipid depletion.[9] Fatostatin decreased activation of the reporter gene with an IC_{50} of 5.6 μM (Figure 2), which is consistent with results of previous studies.[9]

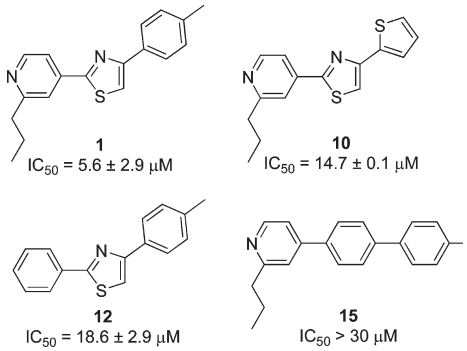

Figure 2. Inhibitory activities of fatostatin (**1**) and analogues **10**, **12**, and **15** against the activation of SREBP in the luciferase reporter assay.

Table 1. Effects of Pyridine Group Substitutions on the Activation of SREBP

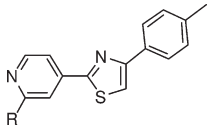

compd	R	IC_{50} (μM)[a]
1	*n*-Pr	5.6 ± 2.9
4a	Et	6.8 ± 3.4
4b	H	>30

[a] All values are the mean ± standard deviation, $n \geq 3$.

Replacement of any one of fatostatin's three aromatic rings with simpler aromatic structures affected activity. For example, **10**, a thiophene substitution, had an IC_{50} of 14.7 μM in the reporter assay (Figure 2). Replacement of the 2-propylpyridine group with phenyl group (**12**) resulted in a 3.3-fold decrease in potency. Analogue **15**, which lacked the central thiazole of fatostatin, showed a large loss of activity, suggesting that the central thiazole moiety is important.

Changing the length of the alkyl chain at the 2-position of pyridine moiety also influenced activity of the fatostatin derivatives. Activity of the ethyl derivative (**4a**) was almost the same as that of fatostatin (Table 1). However, removal of *n*-propyl group (**4b**) resulted in reduced activity, suggesting that a lipophilic alkyl group at this position is essential.

The methyl group of toluene is often oxidized in vivo by cytochrome P450. Therefore, the effects of substitutions of the toluene moiety of fatostatin were examined (**5**−**9** and **16**−**18**). Removal of the methyl group in the toluene moiety (**5a**) led to a 4-fold decrease in potency (Table 2). Halogen substitutions (**5b**−**d**), which are likely to be more metabolically stable than fatostatin, showed moderate activity. Incorporation of a large benzoyl group (**6**) resulted in potency similar to that of the halogenated derivatives. Hydrophilic substitutions, such as hydroxy and methoxy groups (**7** and **16**) also failed to increase activity.

Effects of substitution at 2- and 3-positions of the benzene ring were also examined. 3-Methoxy, 3-hydroxy, and 2-hydroxy derivatives (**8**, **17**, and **18**) were less potent than fatostatin. However, the 2-methoxy derivative (**9**) exhibited a slight increase in activity

dx.doi.org/10.1021/jm200304y | J. Med. Chem. 2011, 54, 4923–4927

Table 2. Effects of Phenyl Group Substitutions on the Activation of SREBP

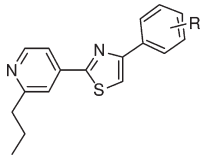

compd	R	IC_{50} (μM)[a]
5a	H	23.0 ± 5.6
5b	4-F	12.4 ± 3.1
5c	4-Cl	10.7 ± 0.9
5d	4-Br	9.8 ± 0.6
6	4-OBz	7.7 ± 1.0
7	4-OMe	13.0 ± 3.3
8	3-OMe	10.2 ± 1.2
9	2-OMe	3.2 ± 0.4
16	4-OH	9.6 ± 1.2
17	3-OH	9.5 ± 0.4
18	2-OH	14.4 ± 0.2

[a] All values are the mean ± standard deviation, $n \geq 3$.

Table 3. Effects of N-Substitution on the Activation of SREBP

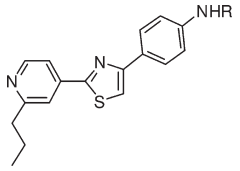

compd	R	IC_{50} (μM)[a]
19	H	8.6 ± 2.0
20	isopropyl	2.8 ± 0.4
21	benzyl	3.0 ± 0.1
22	methylcyclopropyl	4.9 ± 3.1
23	acetyl	7.1 ± 1.5
24	methansulfonyl	0.7 ± 0.2
25	thiophenesulfonyl	0.9 ± 0.5
26	tosyl	2.3 ± 0.0
27	*tert*-butoxycarbonyl	1.9 ± 0.2
25-hydroxycholesterol		0.3 ± 0.0

[a] All values are the mean ± standard deviation, $n \geq 3$.

(Table 2), suggesting that substitution of the toluene moiety of fatostatin might further optimize potency and aqueous solubility. Therefore, further efforts were focused on substitution at the 4-position of the toluene moiety.

A variety of basic amine groups were introduced in the 4-position of the toluene moiety. The potency of an aniline derivative (**19**) was similar to that of fatostatin, and secondary amine derivatives (**20**−**22**) showed slight improvement in activity (Table 3). Introduction of amide (**23**) or carbamate (**27**)[9] did not significantly improve potency; however, addition of sulfonamide (**24**−**26**) increased activity. Analogue **24**, with methanesulfonamide, exhibited the most potent activity: an IC_{50} of 0.7 μM,

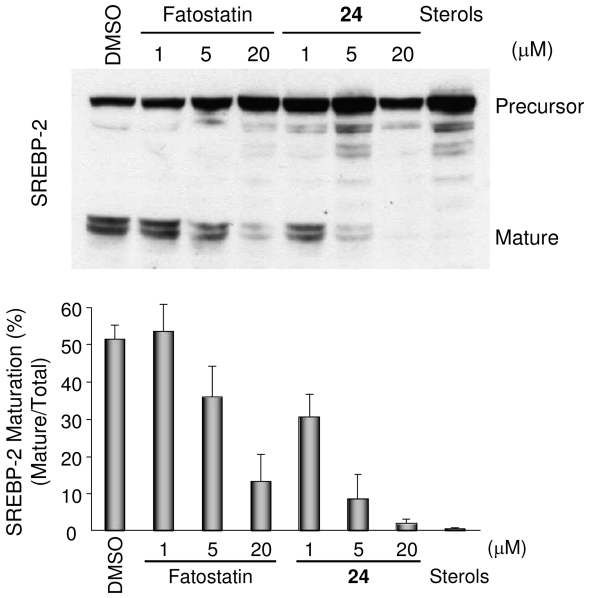

Figure 3. Effects of fatostatin (**1**) and **24** on the proteolytic activation of SREBP-2 in cells. Top: Western blot analysis of SREBP-2. CHO-K1 cells were treated with 1% (v/v) DMSO (vehicle), varied concentrations (1, 5, and 20 μM) of fatostatin (**1**) or **24**, or sterols (10 μg mL^{-1} cholesterol or 1 μg mL^{-1} 25-hydroxycholesterol). The precursor and mature forms of SREBP-2 were detected by an SREBP-2 antibody. The positions of the precursor and mature forms of SREBP-2 are indicated. Bottom: Quantification of the Western blot analysis. Percentages of the mature form of SREBP-2 are shown. Values are the mean ± SD of three independent experiments.

comparable to the potency of endogenous inhibitor 25-hydroxycholesterol, which had an IC_{50} of 0.3 μM.[12]

The inhibition of SREBP activation mediated by **24** was confirmed by Western blot analysis of SREBP-2 (Figure 3). Treatment of the CHO-K1 cells with **24** decreased the percentage of the mature form of SREBP-2 (68 kDa) at lower concentrations than treatment with fatostatin. Densitometric analysis of the gels indicated that the IC_{50} of **24** was ~1 μM, which is 5−10 times lower than the IC_{50} of fatostatin (~10 μM). The IC_{50} values were consistent with the values obtained via the reporter gene assays.

Fatostatin selectively down-regulates endogenous SREBP-responsive genes in cultured human prostate cancer cells.[9] Real-time RT-PCR analysis of nine representative SREBP-responsive genes[13] was carried out to determine the selectivity of analogue **24**. Transcription of all nine genes was down-regulated by at least 25% (Figure 4). In contrast, treatment with **24** had no significant effect on transcription of three control genes unrelated to SREBP. Thus, the mode of action of **24** appears to be similar to that of fatostatin.

The in silico properties calculated for fatostatin and analogues **20** and **24** suggested that **24** has potential for further pharmaceutical development (see Supporting Information, Table S1). Typically, compounds that violate one or more of the "rule-of-five" (molecular weight of >500 Da, log P > 5, more than 5 H-bond donors, and more than 10 H-bond acceptors) are poorly absorbed.[14] Fatostatin and **20** violated one "rule-of-five"; their clogP values were 5.72 and 5.82, respectively. Analogue **24** had a clogP of 3.97 and a polar surface area of 108.57 $Å^2$. As expected, the in vitro aqueous solubility of **24** at pH 7 was more than 10 times higher than that of fatostatin or **20** (Table 4).

dx.doi.org/10.1021/jm200304y |*J. Med. Chem.* 2011, 54, 4923–4927

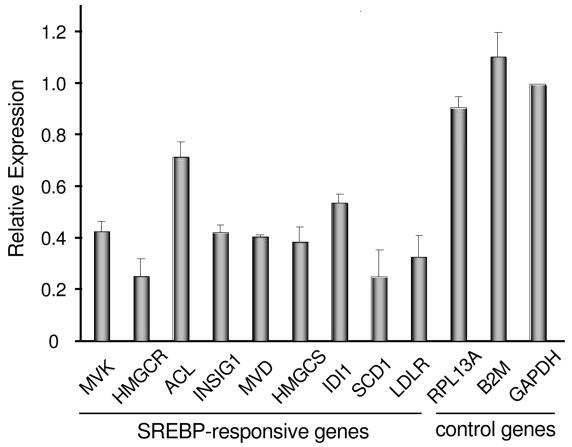

Figure 4. Effects of **24** on the expression of SREBP-responsive genes in DU145 cells: MVK, mevalonate kinase; HMGCR, HMG-CoA reductase; ACL, ATP citrate lyase; INSIG1, insulin induced gene 1; MVD, mevalonate pyrophosphate decarboxylase; HMGCS, HMG-CoA synthase 1; IDI1, isopentenyl diphosphate δ isomerase 1; SCD1, stearoyl-CoA desaturase; LDLR, LDL receptor; RPL13A, ribosomal protein L13a; B2M, β-2 microglobulin; GAPDH, glyceraldehyde 3-phosphate dehydrogenase. Values are the mean ± SD of two independent experiments.

Table 4. In Vitro Aqueous Solubility at pH 3 and 7

compd	solubility, pH 3 (μM)	solubility, pH 7 (μM)
1	80.0	2.0
20	>225	3.0
24	>225	33.0

We examined other physicochemical properties of fatostatin and analogues **20** and **24**. The intrinsic clearance rates measured in mouse hepatocytes were 606, 272, and 137 mL min^{-1} kg^{-1}, respectively, and the corresponding half-lives ($t_{1/2}$) were 10.1, 22.4, and 44.4 min. Although fatostatin and **20** showed low metabolic stability in mouse hepatocytes, **24** was moderately stable.

Results of parallel artificial membrane permeability assays (PAMPA) indicated that passive permeability through an artificial membrane was low for fatostatin, moderate for **20**, and high for **24** (Table 5). Thus, **24** is likely to have greater permeability in vivo than fatostatin or **20**. Warfarin (10 μM) was used as a control for the integrity of membrane. Retention of all compounds within the membrane was greater than 90%, probably because of the high lipophilicity of the compounds.

We previously demonstrated that intraperitoneal injection of fatostatin blocked increases in body weight, blood glucose, and hepatic fat accumulation in obese ob/ob mice, even under conditions of uncontrolled food intake.[9] However, fatostatin was not suited for oral administration and further animal studies. To demonstrate oral availability of **24**, we provided ob/ob mice with ad libitum access over an 8-week period to normal chow that contained **24**. The **24**-treated chow was fed at a dose rate calculated to provide about 0.7 mg of **24** per day, at about 23 mg/kg body weight, to 5-week-old male ob/ob mice weighing an average of ~30 g. After 8 weeks on the **24**-treated chow, the mice gained 8−9% less weight than control mice, which were fed the same chow minus the compound (37.9 ± 0.9 vs 41.4 ± 1.1 g/mouse, respectively) (Table 6). Food intake was slightly lower in the treated mice compared to controls (3.4 ± 0.54 vs 3.6 ± 0.54 g/mouse per day). Blood glucose was lower in the treated mice vs

Table 5. PAMPA Permeability Results for Fatostatin (1) and Analogues 20 and 24

compd	PAMPA P_{app} (10^{-6} cm/s)	% membrane retention	ref	ref PAMPA P_{app} (10^{-6} cm/s)	ref % membrane retention
1	0.7555	94	warfarin	4.11	0
20	1.059	93.95	warfarin	5.34	0
24	14.98	97.35	warfarin	5.58	0

Table 6. Effect of Feeding ob/ob Mice Analogue 24[a]

	control	treated
body weight (g/mouse)	41.4 ± 1.1	37.9 ± 0.9*
glucose (mg/dL)	243.7 ± 27.6	214 ± 16#
cholesterol (dL)	285 ± 8	220 ± 11*
HDL (mg/dL)	164.83 ± 4.5	164.5 ± 5.3
LDL (mg/dL)	79.38 ± 2.85	50.2 ± 4.4*
TG in liver (mg/g tissue)	42 ± 2	28 ± 1*

[a] Male ob/ob mice were fed either normal chow (controls) or normal chow with **24** for 8 weeks. Body weight and food intake were monitored and recorded daily. At the end of the experiments, serum constituents were determined and TG levels in liver were determined as we described previously.[9] HDL, high-density lipoprotein; LDL, low-density lipoprotein; TG, triglycerides. Values are the mean ± SE (n = 10): (*) $P < 0.05$; (#) $P = 0.09$.

controls (214 ± 16 vs 243.7 ± 27.6 mg/dL) (Table 6). The serum level of total cholesterol was lower in the treated mice compared to controls (220 ± 11 vs 285 ± 8 mg/dL). There was a ~37% decrease in the level of LDL in the serum of treated mice compared to controls (50.2 ± 4.4 vs 79.38 ± 2.85 mg/dL); however, no detectable change was observed in the HDL level in the serum of treated mice compared to controls (164.5 ± 5.3 vs 164.83 ± 4.5 mg/dL) (Table 6). The triglyceride level in the liver tissues was significantly lower in the treated mice compared to controls, suggesting fatty liver conditions were ameliorated in the treated group (28 ± 1.0 vs 42 ± 2.0 mg/g tissue). These results indicate that **24** is orally available in mice.

Overall, **24**, a methanesulfonamide derivative of fatostatin, exhibited the highest activity in a cell-based assay and exhibited better in vitro and in vivo physicochemical properties than fatostatin or the other derivatives that were synthesized and evaluated. Analogue **24** (FGH10019) is the most appropriate molecule for further testing in animal models, and this testing is currently underway.

EXPERIMENTAL SECTION

General. The general chemistry, experimental details, and syntheses of all other compounds are described in the Supporting Information. All tested compounds were >95% pure, as determined by LC (wavelength 235 nm) (Table S2) and/or combustion analysis (Table S3).

4-(2-Methoxyphenyl)-2-(2-propylpyridin-4-yl)thiazole (9). A mixture of prothionamide (**3**) (700 mg, 3.88 mmol) and 2-bromo-1-(2-methoxyphenyl)ethanone (890 mg, 3.89 mmol) in ethanol (15 mL) was stirred for 0.5 h at 80 °C, then cooled to 0 °C. The yellow precipitate was filtered off and washed with cold ethanol. The residue was partitioned between EtOAc and saturated $NaHCO_3$ solution. The aqueous phase was extracted with EtOAc. The combined extracts were dried over Na_2SO_4 and concentrated to produce **9** (742 mg, 62%) as a yellow foam. ^{1}H NMR (300 MHz, $CDCl_3$): δ 8.60 (d, J = 5.2 Hz, 1H),

8.38 (d, J = 7.7 Hz, 1H), 8.06 (s, 1H), 7.78 (s, 1H), 7.71 (d, J = 5.2 Hz, 1H), 7.33 (t, J = 7.7 Hz, 1H), 7.09 (t, J = 7.7 Hz, 1H), 7.01 (d, J = 7.7 Hz, 1H), 3.95 (s, 3H), 2.87 (t, J = 7.7 Hz, 2H), 1.83 (m, 2H), 1.00 (t, J = 7.4 Hz, 3H). m/z = 311 $[M + H]^+$. Anal. ($C_{18}H_{18}N_2OS$) C, H, N, S.

***N*-Isopropyl-4-(2-(2-propylpyridin-4-yl)thiazol-4-yl)aniline (20).** Acetone (2.5 mL, 34.5 mmol) and acetic acid (2.0 mL, 34.5 mmol) were added to a stirred solution of **19** (1.02 g, 3.45 mmol) in CH_2Cl_2 (20 mL). After the mixture was stirred for 1 h, $Na(AcO)_3BH$ (1.5 g, 6.9 mmol) was added. The mixture was stirred for 20 h. The mixture was poured into saturated $NaHCO_3$ solution and extracted with EtOAc. The combined extracts were dried over Na_2SO_4 and concentrated. Chromatography of the crude product (SiO_2, 4:1 hexane/EtOAc) produced **20** (845 mg, 73%) as a white foam. ^{1}H NMR (300 MHz, $CDCl_3$): δ 8.61 (d, J = 5.2 Hz, 1H), 7.81 (d, J = 8.5 Hz, 2H), 7.76 (d, J = 1.4 Hz, 1H), 7.68 (dd, J = 1.4, 5.2 Hz, 1H), 7.34 (s, 1H), 6.65 (d, J = 8.5 Hz, 2H), 3.70 (m, 1H), 2.86 (t, J = 7.6 Hz, 2H), 1.83 (m, 2H), 1.25 (d, J = 6.0 Hz, 6H), 1.02 (t, J = 7.4 Hz, 3H). m/z = 338 $[M + H]^+$. Anal. ($C_{20}H_{23}N_3S$) C, H, N, S.

***N*-(4-(2-(2-Propylpyridin-4-yl)thiazol-4-yl)phenyl)methanesulfonamide (24).** Methanesulfonyl chloride (0.23 mL, 2.97 mmol) was added to a stirred solution of **19** (800 mg, 2.71 mmol) and pyridine (0.66 mL, 8.1 mmol) in CH_2Cl_2 (20 mL) at 0 °C. After being stirred for 0.5 h, the mixture was poured into 2 M citric acid solution and extracted with EtOAc. The combined extracts were washed with saturated $NaHCO_3$ solution and brine, dried over Na_2SO_4, and concentrated to produce **24** (880 mg, 87%) as a yellow foam. ^{1}H NMR (300 MHz, CD_3OD): δ 8.55 (d, J = 5.2 Hz, 1H), 8.02 (d, J = 8.8 Hz, 2H), 7.95 (s, 1H), 7.90 (d, J = 1.9 Hz, 1H), 7.84 (dd, J = 1.9, 5.2 Hz, 1H), 7.34 (d, J = 8.8 Hz, 2H), 3.00 (s, 3H), 2.86 (t, J = 7.7 Hz, 2H), 1.80 (m, 2H), 1.01 (t, J = 7.3 Hz, 3H). m/z = 374 $[M + H]^+$. Anal. ($C_{18}H_{19}N_3O_2S_2$) C, H, N, S.

■ ASSOCIATED CONTENT

Supporting Information. Schemes S1−S3; synthesis details of **4**−**8**, **10**, **12**, **15**−**18**, **21**−**23**, **25**, and **26**; biological assay methods; HPLC and combustion data. This material is available free of charge via the Internet at http://pubs.acs.org.

■ AUTHOR INFORMATION

Corresponding Author

*For S.J.W.: phone, 713-798-4783; fax, 713-796-9438; e-mail, swakil@bcm.edu. for M.U.: phone, +81-774-38-3225; fax, +81-774-38-3226; e-mail, uesugi@scl.kyoto-u.ac.jp.

Present Addresses

§Ewha Woman's University, Seoul 120-750, Korea.

Notes

L.A.-E., S.J.W., and M.U. have interests in FGH Biotech, Inc., a Houston-based company that exclusively licensed the technology described in this manuscript.

■ ACKNOWLEDGMENT

This work was supported in part by grants to M.U. from the Hoh-ansha Foundation and MEXT (Grant-in-Aid 21310140) and by grants to S.J.W. from the Hefni Technical Training Foundation and the National Institutes of Health (Grant GM-63115). We also thank J. Sakai for an SREBP-2 antibody and a reporter gene construct, and T. Orihara, T. Morii, and T. Hasegawa for experimental support. S.K. is a postdoctoral fellow of JSPS. The Kyoto research group participates in the Global COE program "Integrated Materials Science" (No. B-09).

■ ABBREVIATIONS USED

SREBP, sterol regulatory element-binding protein; S1P, site-1 protease; S2P, site-2 protease; SCAP, SREBP cleavage-activating protein; CHO-K1, Chinese hamster ovary K1; PAMPA, parallel artificial membrane permeability assay; MVK, mevalonate kinase; HMGCR, HMG-CoA reductase; ACL, ATP citrate lyase; INSIG1, insulin-induced gene 1; MVD, mevalonate pyrophosphate decarboxylase; HMGCS1, HMG-CoA synthase 1; IDI1, isopentenyl diphosphate δ isomerase 1; SCD1, stearoyl-CoA desaturase; LDLR, low-density lipoprotein receptor; RPL13A, ribosomal protein L13a; B2M, β-2 microglobulin; GAPDH, glyceraldehyde 3-phosphate dehydrogenase; HDL, high-density lipoprotein; TG, triglycerides

■ REFERENCES

(1) Brown, M. S.; Goldstein, J. L. The SREBP pathway: regulation of cholesterol metabolism by proteolysis of a membrane-bound transcription factor. *Cell* **1997**, *89*, 331–340.

(2) Osborne, T. F. Sterol regulatory element-binding proteins (SREBPs): key regulators of nutritional homeostasis and insulin action. *J. Biol. Chem.* **2000**, *275*, 32379–32382.

(3) Sakai, J.; Duncan, E. A.; Rawson, R. B.; Hua, X.; Brown, M. S.; Goldstein, J. L. Sterol-regulated release of SREBP-2 from cell membranes requires two sequential cleavages, one within a transmembrane segment. *Cell* **1996**, *85*, 1037–1046.

(4) Goldstein, J. L.; DeBose-Boyd, R. A.; Brown, M. S. Protein sensors for membrane sterols. *Cell* **2006**, *124*, 35–46.

(5) Hua, X.; Nohturfft, A.; Goldstein, J. L.; Brown, M. S. Sterol resistance in CHO cells traced to point mutation in SREBP cleavage-activating protein. *Cell* **1996**, *87*, 415–426.

(6) Radhakrishnan, A.; Sun, L. P.; Kwon, H. J.; Brown, M. S.; Goldstein, J. L. Direct binding of cholesterol to the purified membrane region of SCAP: mechanism for a sterol-sensing domain. *Mol. Cell* **2004**, *15*, 259–268.

(7) Yang, T.; Espenshade, P. J.; Wright, M. E.; Yabe, D.; Gong, Y.; Aebersold, R.; Goldstein, J. L.; Brown, M. S. Crucial step in cholesterol homeostasis: sterols promote binding of SCAP to INSIG-1, a membrane protein that facilitates retention of SREBPs in ER. *Cell* **2002**, *110*, 489–500.

(8) Choi, Y.; Kawazoe, Y.; Murakami, K.; Misawa, H.; Uesugi, M. Identification of bioactive molecules by adipogenesis profiling of organic compounds. *J. Biol. Chem.* **2003**, *278*, 7320–7324.

(9) Kamisuki, S.; Mao, Q.; Abu-Elheiga, L.; Gu, Z.; Kugimiya, A.; Kwon, Y.; Shinohara, T.; Kawazoe, Y.; Sato, S.; Asakura, K.; Choo, H. Y.; Sakai, J.; Wakil, S. J.; Uesugi, M. A small molecule that blocks fat synthesis by inhibiting the activation of SREBP. *Chem. Biol.* **2009**, *16*, 882–892.

(10) Comins, D. L.; Mantlo, N. B. Regiospecific alpha-alkylation of 4-chloro(bromo)pyridine. *J. Org. Chem.* **1985**, *50*, 4410–4411.

(11) Bilgin, A. A. 2-Pyridylthiazoles II, synthesis and structure elucidations. *Acta Pharm. Turcica* **1988**, *30*, 133–138.

(12) Adams, C. M.; Reitz, J.; De Brabander, J. K.; Feramisco, J. D.; Li, L.; Brown, M. S.; Goldstein, J. L. Cholesterol and 25-hydroxycholesterol inhibit activation of SREBPs by different mechanisms, both involving SCAP and Insigs. *J. Biol. Chem.* **2004**, *279*, 52772–52780.

(13) Horton, J. D.; Shah, N. A.; Warrington, J. A.; Anderson, N. N.; Park, S. W.; Brown, M. S.; Goldstein, J. L. Combined analysis of oligonucleotide microarray data from transgenic and knockout mice identifies direct SREBP target genes. *Proc. Natl. Acad. Sci. U.S.A.* **2003**, *100*, 12027–12032.

(14) Lipinski, C. A.; Lombardo, F.; Dominy, B. W.; Feeney, P. J. Experimental and computational approaches to estimate solubility and permeability in drug discovery and development settings. *Adv. Drug Delivery Rev.* **1997**, *23*, 3–25.